Pion Decay-Mode Tagging in a Plastic Scintillator Using COPPER 500-MHz FADC

著者	田窪　洋介
journal or publication title	IEEE Transactions on Nuclear Science
volume	54
number	4
page range	1222-1226
year	2007
URL	http://hdl.handle.net/10097/46203

doi: 10.1109/TNS.2007.901220

Pion Decay-Mode Tagging in a Plastic Scintillator Using COPPER 500-MHz FADC

Kaoru Yamada, Makoto Yoshida, Youichi Igarashi, Masaharu Aoki, Kazuya Tauchi, Masahiro Ikeno, Yosuke Takubo, Akira Muroi, Manobu Tanaka, and Yoshitaka Kuno

***Abstract*—The PIENU experiment is going to be carried out at TRIUMF to measure the ratio of pion decay rates, $R = \Gamma(\pi^+ \rightarrow e^+\nu_e)/\Gamma(\pi^+ \rightarrow \mu^+\nu_\mu)$, to an accuracy of 0.1%. In order to achieve this goal, a muon identification with waveform analysis in a target scintillator is necessary. Due to the short lifetime of pions, muon pulses tend to overlap onto the tail of pion pulses. Thus waveform analysis with a high frequency flash-ADC is essential for the identification and separation of muon pulses. We use the 500-MHz flash-ADC of the COmmon Pipelined Platform for Electronics Readout system, which was developed at KEK, to readout waveforms from the target scintillator. Muon pulse identification capability of this flash-ADC system was investigated by artificial pulses simulating photomultiplier signals.**

***Index Terms*—COmmon Pipelined Platform for Electronics Readout (COPPER), flash-ADC (FADC), muon, PIENU, pion, waveform.**

I. Introduction

The PIENU experiment (TRIUMF-E1072) is going to be carried out in 2008 at TRIUMF to measure the ratio of pion decay rates, $R = \Gamma(\pi^+ \rightarrow e^+\nu_e)/\Gamma(\pi^+ \rightarrow \mu^+\nu_\mu)$, to an accuracy of 0.1% [1]. This experiment will be very sensitive to pseudo-scalar type new interactions beyond the Standard Model of particle physics.

Beam pions with momentum of about 75 MeV/c will be stopped in a target plastic-scintillator (about $50 \text{ mm} \times 50 \text{ mm} \times 10 \text{ mm}^t$). In most cases, pions decay to muons which subsequently decay to positrons in the target ($\pi \rightarrow \mu \rightarrow e$), however, in some cases, they will decay directly to positrons ($\pi \rightarrow e$). Positrons from the decay chain $\pi \rightarrow \mu \rightarrow e$ have a continuous energy distribution from 0 to 52.8 MeV while positrons from the decay $\pi \rightarrow e$ have monochromatic energy at 69.3 MeV. Positron energy measurement with NaI(Tl) calorimeter can therefore be used for the selection of these decay modes. However, in order to reduce the systematic error to less than 0.1%, additional decay-mode tagging methods independent of the positron energy will be necessary.

One of the additional decay-mode tagging methods is to identify $\pi \rightarrow \mu$ decays in the target by observing the second pulses produced by muons. Due to the short lifetime (26 ns) of pions, muon pulses overlap with the preceding pion pulses in most cases. In a previous experiment [2] performed at TRIUMF, two ADCs with different gate widths (one seeing whole pulse and the other seeing only the earlier component of the first pulse) were used. However, in this experiment, the waveform of the photomultiplier signal from the target will be recorded by a waveform digitizing system. In order to fulfill the experimental requirements of PIENU, second pulses from muons need to be detected if the pulses originate more than ~2 ns after pion pulses.

A waveform digitizer has been used in a similar way for pion tagging in BNL/E787 to identify $\pi \rightarrow \mu$ decays [3], [4]. It was reported that $\pi \rightarrow \mu$ pulses could be detected and "selected" as close as 8 ns after the previous pion pulse. In contrast, in the PIENU experiment, the waveform will be used for "rejecting" the $\pi \rightarrow \mu$ decays. The difference between those two applications, selection and rejection, will be significant. It is possible to detect $\pi \rightarrow \mu$ decays much closer to pion pulses when simply attempting to reject them.

II. COPPER System and 500-MHz Flash-ADC Module

The waveform digitization system employed for the PIENU experiment is based on the COPPER platform. The COmmon Pipelined Platform for Electronics Readout (COPPER) was developed by KEK mainly for Belle and experiments at the J-PARC facility [5]. The main board of COPPER is a 9U-size VME board with local extensions specific to COPPER called KEK-VME specification. Each main board has four slots to install front-end modules (FINESSE) for signal digitization, and three PCI mezzanine card (PMC) slots for on-board data processing, triggering and other purposes.

The major advantage of the COPPER system is its on-board data processing capability. It can be equipped with a processor board running Linux. Data obtained from the FINESSE modules are transferred to the on-board processor via a high-speed (80 MB/s) internal bus. Data can be processed before they are transmitted to a host computer outside the main board. This is advantageous compared to other commercially available flash-ADC (FADC) systems such as CAEN V1721 and Acqiris DC271. The other merit of the COPPER system is its cost; the cost per channel is less than half of those commercially available.

The 500-MHz FADC module that will be used in the PIENU experiment was originally developed for other experiments and meets the FINESSE specification. Fig. 1 shows the FADC FINESSE module used for this study. There are two channels of analog inputs on a single module. Two 250-MHz FADC devices (Fairchild SPT7721SI) are driven in alternating phases in order

Manuscript received December 27, 2006; revised May 1, 2007. This work was supported by Grant-in-Aids for Scientific Research from the Japan Society for the Promotion of Science (JSPS).

K. Yamada, M. Yoshida, M. Aoki, Y. Takubo, A. Muroi and Y. Kuno are with Osaka University, Toyonaka, Osaka 560-0043, Japan (e-mail: yamada@kuno-g.phys.sci.osaka-u.ac.jp).

Y. Igarashi, K. Tauchi, M. Ikeno and M. Tanaka are with the High Energy Accelerator Research Organization (KEK), Tsukuba, Ibaraki 305-0801, Japan.

Digital Object Identifier 10.1109/TNS.2007.901220

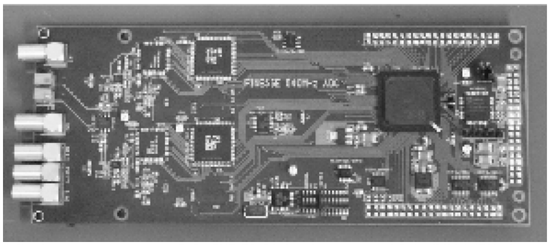

Fig. 1. The 500-MHz flash-ADC module for COPPER system.

to realize 500-MHz sampling. This device has a resolution of 8 bits and a dynamic range of ± 500 mV. According to the specification sheet, the effective number of bits (ENOB) is about 6.5 bits. The non-linearity of the FADC is less than 1%. The dynamic range of the module can be adjusted from a range of $-1000 \sim 0$ mV to a range of $0 \sim +1000$ mV by an external circuit.

Two or three COPPER main boards with 500-MHz FADC FINESSE modules installed in all peripheral slots (24 channels in total) will be used in the experiment for recording all plastic scintillator signals. The time window to be recorded is about 8 μs for all channels in order to be able to detect beam pileups.

III. Setup

Pions are available only in a limited number of facilities, and the time length for pion usage is limited in many of those facilities. For this reason, in our study, we used electrically generated analog pulses to simulate pion signals. The simulated pulses were produced by feeding step pulses to a simple capacitor-and-resistor shaping circuit. The pulse shape was adjusted to simulate a signal from a plastic scintillation counter read by a Hamamatsu H1949 photomultiplier (PMT). Fig. 2 shows a comparison of the real PMT signal and the simulated signal. The rise time is about 3 ns and the decay time is about 10 ns. The simulated signal reproduces the real PMT signal accurately.

A block diagram for this measurement is illustrated in Fig. 3. Two FINESSE modules were used to test synchronous operation. A 240-MHz sampling clock was fed into the FINESSE modules. We used 240-MHz instead of 250-MHz since the maximum frequency of the clock generator used in this study was limited. The simulated pulse signal was split into two paths. The first was directly fed to a linear amplifier, and the second was attenuated and delayed to simulate a $\pi \rightarrow \mu$ signal. This was then added to the main pulse by the linear amplifier. The second pulse was not used for the single pulse study.

IV. Single-Pulse Study

A single-pulse study was performed to collect pulse shape information. The pulse height of the simulated PMT signal was set at -640 mV, and the pulse shape was recorded with the 500-MHz FADC. The pulse shape data were obtained by changing the relative timing between the simulated pulses and the sampling clock in 100 ps steps. As a result, the discrete template of the pulse shape was obtained in 100 ps intervals, which is more precise than the sampling period of the FADC system itself. From this, a continuous template of the pulse shape, $F(t)$, was defined by interpolating the discrete template.

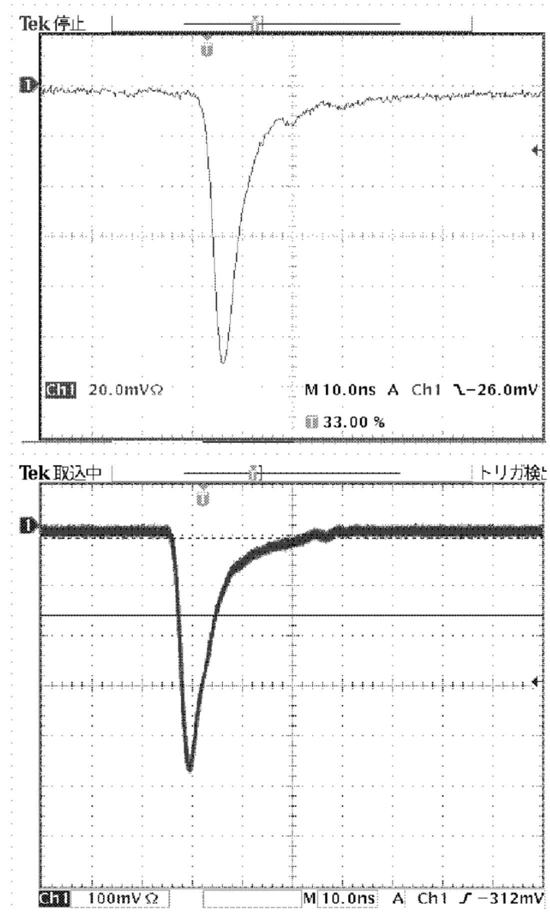

Fig. 2. Upper: a real PMT signal from the plastic scintillator. Lower: a simulated signal by the shaper circuit.

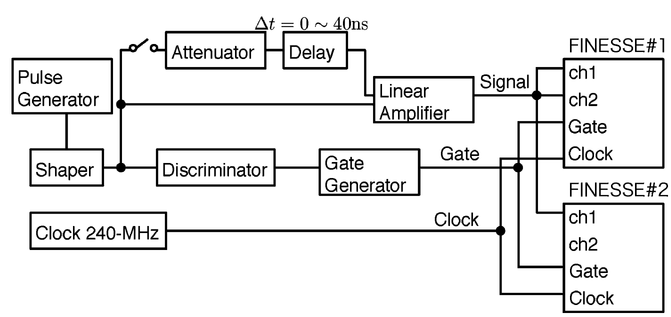

Fig. 3. Setup of the study. A switch was off for the single pulse study and was on for the double pulse study.

In order to verify the goodness of $F(t)$, a pulse fitting of the single pulse was performed. The fitting function used was $V(A_1, T_1; t) = A_1 F(t + T_1)$, where A_1 and T_1 are both free parameters. The χ^2 of the pulse fitting is defined as

$$\chi^2 = \sum_{i=1}^{40} \frac{\left(V_i^{\mathrm{FADC}} - V(A_1, T_1; t_i)\right)^2}{\sigma^2} \tag{1}$$

where i denotes the sequential numbering of the FADC sample points, V_i^{FADC} is the FADC readout value at sample point i, t_i is the time of the sample point i, and σ is the voltage resolution of the FADC presumably including the effect of electrical noise.

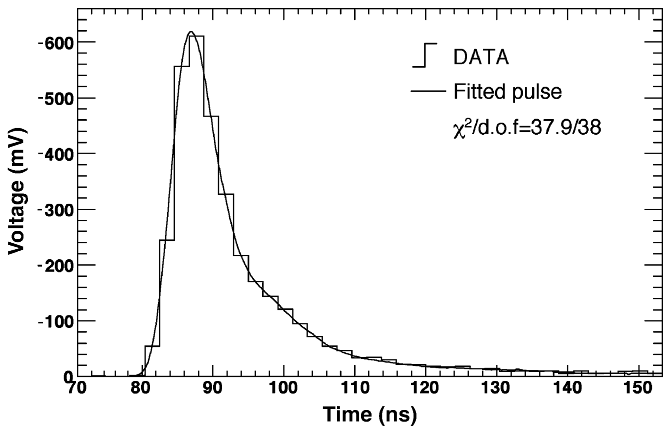

Fig. 4. Typical result of the single-pulse fitting to the single-pulse data.

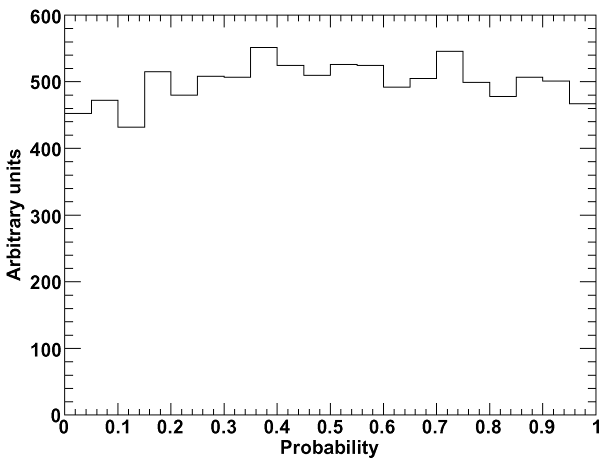

Fig. 5. The probability distribution of the single-pulse fitting.

The number of sample points incorporated was 40 bins (80 ns) starting from 9 bins before the peak bin of the pulse. The best possible fit was obtained by searching the set of free parameters (A_1, T_1) for those which give the minimum value of the χ^2. This minimization process is well established. We used the MINUIT software package [6] in this study. The initial values of the free parameters for the fit with MINUIT were set to the pulse height and the timing of the peak bin of the pulse.

Fig. 4 shows a typical result of the fitting procedure. The standard deviation σ was adjusted so that the χ^2 distribution becomes consistent with an ideal distribution of χ^2 for degree-of-freedom (d.o.f) being 38, and it is $\sigma = 2.33$ mV, which corresponds to 6.9 of ENOB. This result is consistent with the ENOB value taken from the specification sheet of the FADC chip. The probability distribution of the χ^2 obtained from the fitting is shown in Fig. 5. The flatness of this probability distribution proves the goodness of our fitting function, $V(A_1, T_1; t)$.

Fig. 6 shows the relative timings of the signals between the 2nd channel of the 1st FINESSE module and the 1st channel of the same FINESSE module (same-FINESSE), and between the 1st channel of the 2nd FINESSE and the 1st channel of the 1st FINESSE (different-FINESSEs), obtained by the single-pulse fitting analysis. The root mean square (r.m.s.) of the distributions are both about 20 ps, which is almost two orders of magnitudes better than the sampling clock interval. The pulse height was set at -640 mV in this study.

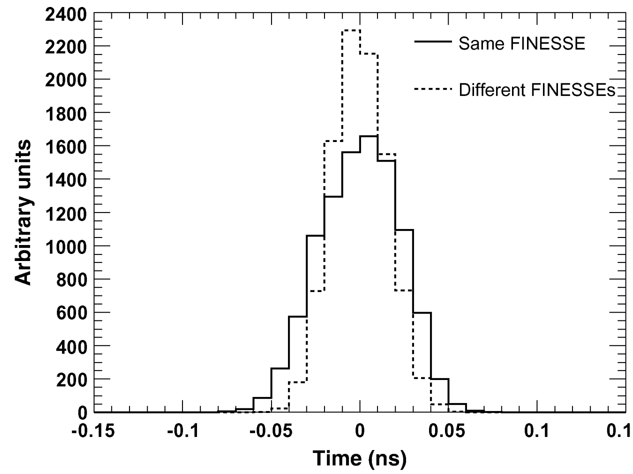

Fig. 6. Relative timing distributions between two channels in the same FINESSE module (solid histogram), and between the different FINESSE modules (dashed histogram).

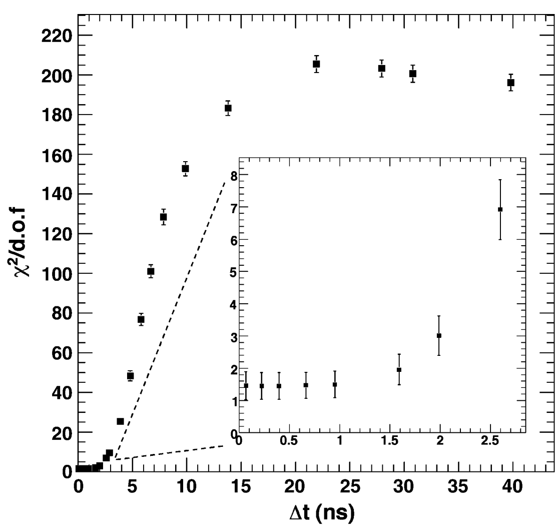

Fig. 7. Reduced χ^2 of the single-pulse fitting to the double pulse data as a function of Δt. Inset shows a close-up for $\Delta t \leq 2.8$. Errors indicate the root mean square of the reduced χ^2 distribution.

V. Double-Pulse Study

Double pulses were produced by turning on the switch in the block diagram (Fig. 3); summing the main pulse and delayed pulse with the linear amplifier. The pulse heights of the main pulse and delayed pulse were fixed at -478 mV and -118 mV respectively, producing a ratio of 4:1. This ratio was modeled on the mean energy deposits of π^+ and μ^+ in a plastic-scintillator target (π^+: 14.6 MeV, μ^+: 4.1 MeV). In order to simulate the random timings of the second pulses in the real experiment, pulse shapes were recorded for different settings of the second pulse delay.

A. Fitting as a Single Pulse

In order to estimate the performance of the detection of the second pulse, the recorded double pulse data were first fitted

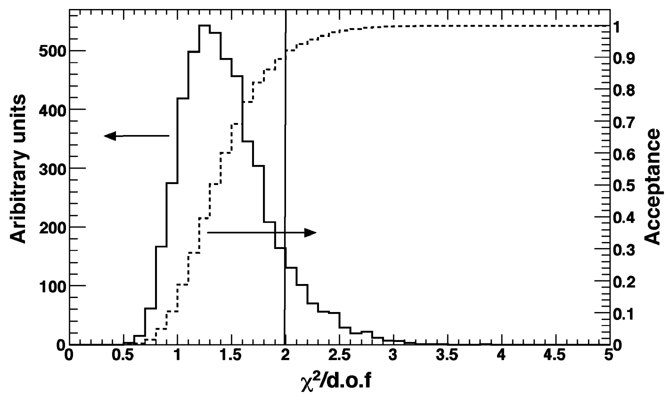

Fig. 8. Reduced χ^2 distribution for the case of $\Delta t = 0$ ns (solid histogram). Acceptance, which is equivalent to the integration of the reduced-χ^2 distribution, to single-pulse events is also shown (dashed histogram). A vertical bar indicates the cut position.

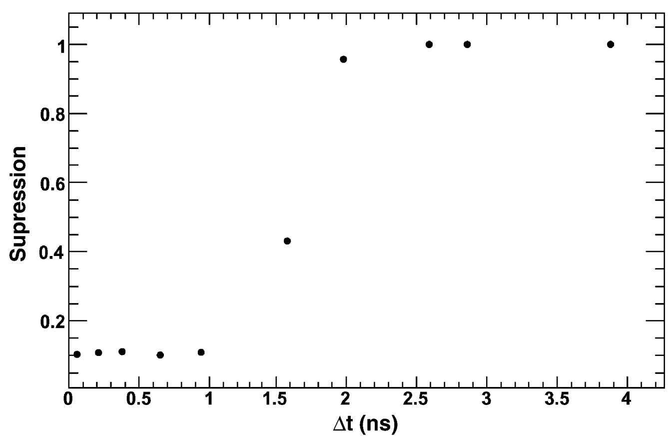

Fig. 9. Double pulse rejection power as a function of Δt. Sizes of error are smaller than the size of points.

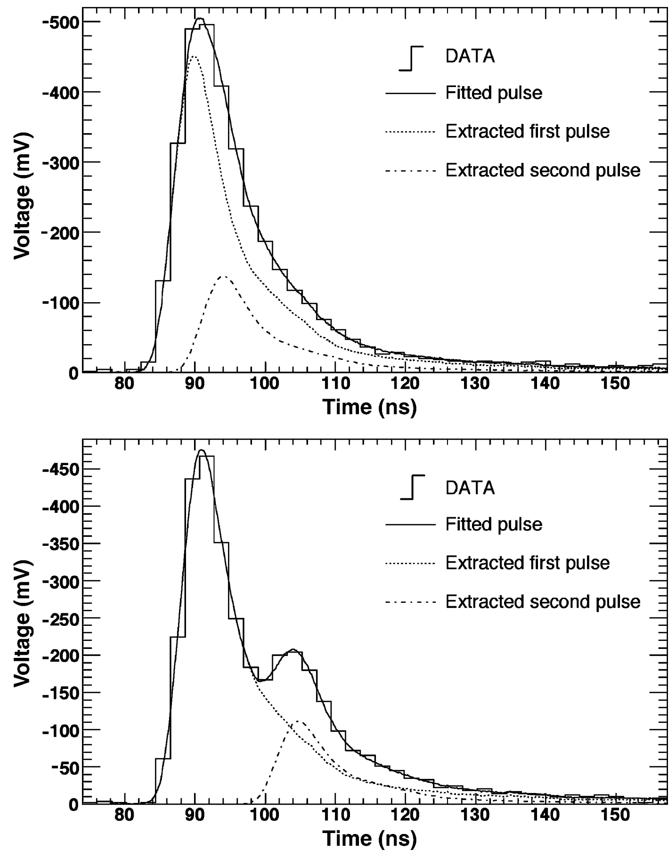

Fig. 10. Typical examples of the double-pulse fitting to the double-pulse data.

with a single pulse function. If the delay of the second pulse is sufficiently large, the combined pulse shape is not consistent with a single pulse, and the χ^2 of the fit should blow up to large value. On the other hand, if the second pulse is close to the main pulse, the pulse shape will look like a single pulse and χ^2 of the fitting should be consistent with a single pulse hypothesis. Therefore, a reduced χ^2 (defined by $\chi^2/d.o.f$) should be a good estimator to reject the double pulse signal as long as the second pulse is not too close to the main pulse. Fig. 7 shows the reduced χ^2 of the single-pulse fitting as a function of second pulse delay (Δt). It is observed that the reduced χ^2 blows up for $\Delta t > 2$ ns. It is worth noting that the reduced χ^2 converges to 1.5 instead of 1 for $\Delta t \to 0$. This might be caused by a non-linearity of the linear amplifier, the attenuator and the cable delay line. However it is not a serious problem as long as the blow-up of the reduced χ^2 can be clearly observed. Note that a pulse template, $F(t)$, for this study was obtained by using a single pulse with pulse height -478 mV.

The rejection condition of the double-pulse signal in the single-pulse fitting method is optimized by requiring 90% acceptance of the proper single-pulse signal, which was determined with data at $\Delta t = 0$. Fig. 8 shows the reduced χ^2 distribution for $\Delta t = 0$. The rejection condition was therefore set at 2 for the reduced χ^2 based on this plot. Fig. 9 shows the rejection performance with this condition (cutting the events with reduced χ^2 being larger than 2), as a function of Δt. The rejection power is almost 100% for $\Delta t \geq 2$ ns.

B. Fitting as a Double Pulse

The double pulse data were fitted with a double-pulse function to extract the pulse information. The double-pulse fitting function is $V(A_1, T_1, A_2, T_2; t) = A_1 F(t+T_1) + A_2 F(t+T_2)$, where the single pulse shape template, $F(t)$, is the same as that used for the single-pulse fitting. There are four free parameters: pulse height A_i and timing T_i for the first pulse $(i = 1)$ and the second pulse $(i = 2)$. The number of sample points incorporated to the fit was 40 bins ($\approx$80 ns) starting from 9 bins before the peak bin of the first pulse. The initial values of the parameters for the first pulse were obtained by single-pulse fitting over a limited number of sample points (11 bins starting from 9 bins before the peak bin of the first pulse). The initial parameters of the second pulse were set by finding the pulse height and the timing in the residual pulse, where the residual pulse was obtained by subtracting the 11-points-single-pulse fitting result from the original pulse. If the residual pulse is too small, which mostly normally only occurs in the case where Δt is small, the initial parameters of the second pulse are set to be the same as the first pulse. The double-pulse fitting procedure is the same to that for single-pulse fitting. It was observed that the reduced χ^2 is almost constant independently of Δt for this case, which demonstrates the validity of the fitting procedure.

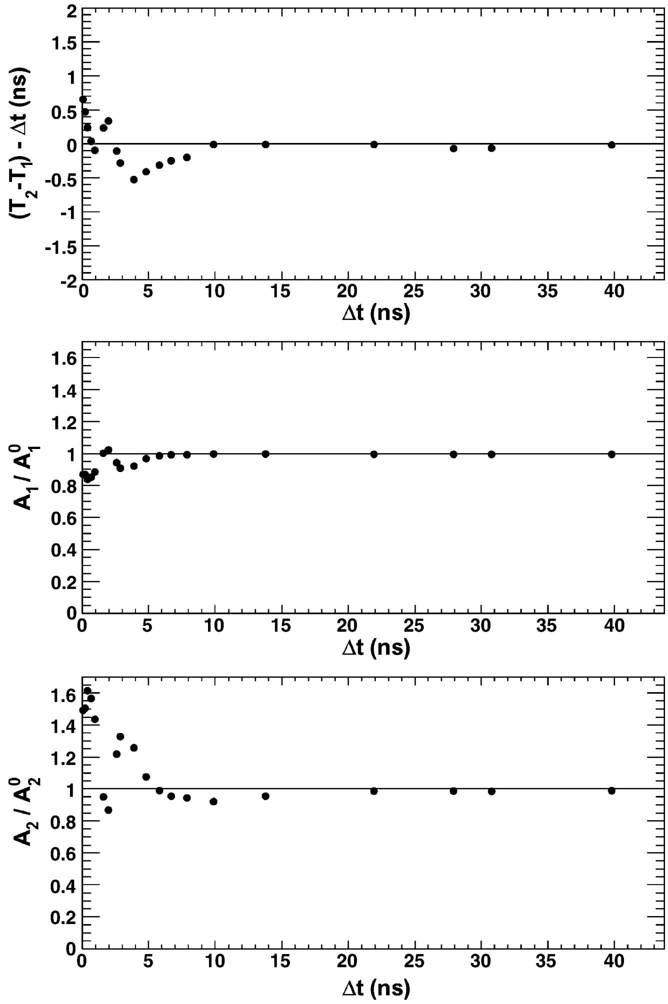

Fig. 11. Deviations of the fitted parameters as a function of Δt. A_is are normalized by A_i^0s, where A_i^0s were obtained by single-pulse fitting before taking sum of two pulses.

Fig. 10 shows typical results of the fitting. Fig. 11 shows the Δt dependence of the fitted results compared to the actual values from the PMT-like pulse generator. It was concluded that the pulse parameters could be obtained with an accuracy of 10% for $\Delta t \geq 5$ ns.

VI. Conclusion

The basic performance of the COPPER 500-MHz FADC was studied by using PMT-like simulated pulses. The timing resolution obtained by the pulse-fitting is about 20 ps(r.m.s) for -640 mV pulse height which is almost two orders of magnitude better than the sampling interval of the FADC. Double pulses can be detected and rejected with almost 100% of efficiency when the second pulse is delayed by 2 ns or more from the first pulse. The pulse heights and timings of each pulse can be extracted with an accuracy better than 10% when the second pulse is delayed by more than 5 ns. These results are impressive considering the moderate performance of the FADC chip itself. It is concluded that the current system is sufficient for rejecting $\pi \rightarrow \mu$ decays in a plastic scintillator for the PIENU experiment.

References

[1] T. Numao and D. A. Bryman *et al.*, "Study of the decay $\pi \rightarrow e\nu$," TRIUMF—Research Proposal 2005.

[2] D. I. Britton *et al.*, "Measurement of the $\pi^+ \rightarrow e^+\nu$ branching ratio," *Phys. Rev. D*, vol. 49, pp. 28–39, 1994.

[3] M. Atiya, M. Ito, J. Haggerty, C. Ng, and F. W. Sippach, "Waveform digitizing at 500 MHz," *Nucl. Instrum. Methods Phys. Res. A*, vol. A279, pp. 180–185, 1989.

[4] D. A. Bryman, J. V. Cresswell, M. LeNoble, and R. Poutissou, "500 MHz transient digitizers based on GaAs CCDs," *IEEE Trans. Nucl. Sci.*, vol. 38, no. 2, pp. 295–300, 1991.

[5] Y. Igarashi *et al.*, "A common data acquisition system for high-intensity beam experiments," *IEEE Trans. Nucl. Sci.*, vol. 52, no. 6, pp. 2866–2871, 2005.

[6] F. James, "Function Minimization and Error Analysis Reference Manual" CERN. Geneva, Switzerland, CERN Program Library Long Writeup D506 [Online]. Available: http://www.asdoc.web.cern.ch/wwwasdoc/minuit/minmain.html